THEORETICAL AND APPLIED MECHANICS
vol. 28-29, pp. 289-324, Belgrade 2002
Issues dedicated to memory of the Professor Rastko Stojanović

Correlation between mechanical and conductive properties of porous/microcracked metals

Igor Sevostianov*

Abstract

Different physical properties of anisotropic porous/microcracked materials - the elastic and the conductive ones, in particular - can be explicitly related to one another. The practical usefulness of such relations lies in the fact that one physical property (say, electric conductivity) may be easier to measure than the other (say, full set of anisotropic elastic constants). Man-made microstructures designed for the optimal *combined* elastic/conductive performance constitute yet another application. These relations, derived from the micromechanical considerations, are confirmed by experiments on several heterogeneous materials. It is also shown that the anisotropic yield surface for a porous ductile material can be constructed from measurements of the effective electric conductivities. The derived cross-property correlations are sensitive to pore aspect ratios and Poisson's ratio of the virgin material.

1 Introduction

Correlations between the effects of microcracks, pores and various inhomogeneities on different physical properties - elastic and conductive, for example - constitute one of the most challenging problems in materials

*Department of Mechanical Engineering, New Mexico State University, Las Cruces, NM 88001, USA (e-mail: igor@saratoga.nmsu.edu)

science. This task is quite challenging: not only the governing equations of elasticity and conductivity are different, but even the tensors that characterize the mentioned properties are of different ranks (fourth rank tensor of elastic moduli vs second rank tensor of conductivity), so that the cross-property correlations should interrelate different numbers of independent components.

Cross-property relations between various effective properties of heterogeneous materials have been examined in several works. The most relevant for the present work is the classical paper of Bristow [1] in which an explicit connection between the effective conductivity and effective elastic moduli of a solid with cracks was derived. The derivation was done in the framework of the non-interaction approximation and for the case of random crack orientations (overall isotropy).

The conductivity - elasticity correlations were further investigated in [2] for the two-phase composites, where the cross-property bounds (that are narrower than the classical Hashin-Shtrikman's ones) were established. These cross-property bounds were substantially advanced by Gibiansky and Torquato [3-5], who narrowed them under additional restrictions on the composite microgeometry and on the properties of constituents. Practical needs of materials science, however, call for the cross-property connections that, preferably,

- have the explicit form;
- can be applied to strongly anisotropic microstructures;
- remain accurate at high contrast between the phases (materials with pores or microcracks)

Relations of this kind were recently obtained in recent works [6-10]. They explicitly interrelated full sets of anisotropic elastic and conductive constants of heterogeneous materials that contain inhomogeneities of diverse shapes and orientations.

The elasticity conductivity relations allow one to go further. In the present paper, it is shown that the anisotropic yield surface for a porous ductile material can be constructed from measurements of the effective electric conductivities. Experimental determination of the yield surface of a ductile material usually requires multiple tests and involves inaccuracies. The procedure is particularly cumbersome in the cases of plastic

anisotropy. The derived yield-conductivity relations allow one to simplify this procedure significantly.

For ductile porous materials, the yield surface was earlier constructed explicitly in terms of the porous space geometry [11], under the following two conditions - restrictions that apply to the present work as well:

- The matrix ("dense") material has a clearly identifiable yield point, followed by a horizontal plateau.
- The porosity does not exceed levels of the order of 15% (beyond this point, the stress-strain curve may lose a clearly identifiable yield point).

However, the information on the porous space required for such a construction - distributions of pore shapes and orientations - may not be readily available (for example, the information on details of the orientational distribution of pores, like the orientational scatter about a certain preferential orientation). The present work expresses the yield surface in terms of conductivities. In particular, this suggests a convenient methodology to construct a (generally anisotropic) yield surface of a porous metal.

It should also be mentioned that correlation between other pairs of effective properties were considered in a number of works. Levin [12] interrelated the effective bulk modulus and the effective thermal expansion coefficient of the two phase isotropic composites. Milton [13] established cross-property bounds for the transport and the optical constants of isotropic composites. Similar bounds for the electrical and the magnetic properties were given by Cherkaev and Gibiansky [14]. The general approach to establishing various cross-property correlations was outlined in [15, 16].

2 Property contribution tensors of an inclusion

In this section we briefly outline the results derived in [7, 17]. We consider a certain reference volume V of an infinite three-dimensional

medium with an inclusion of volume V^*- a region possessing elastic/conductive properties different from the ones of the surrounding material. The properties of the inclusion and of the matrix will be denoted by an asterisk and by "0", respectively.

2.1 Compliance contribution tensors

The compliance contribution tensor $\mathbf{H}$ of an inclusion is defined by the following relation for the overall strain per volume V:

$$\varepsilon_{ij} = S^0_{ijkl}\sigma_{kl} + H_{ijkl}\sigma_{kl} \tag{2.1}$$

where the second term represents the strain change $\Delta\varepsilon_{ij}$due to the presence of the inclusion. $\mathbf{H}$ - tensor depends on the inclusion shape and its elastic properties. ($\mathbf{S}^0$ is the matrix compliance tensor and σ is the "remotely applied" stress, assumed to be homogeneous in the absence of the inclusion). $\mathbf{H}$ - tensor is related to Eshelby's tensor s as follows [7]:

$$\mathbf{H} = \frac{V_*}{V}\left[\mathbf{C}^0 : (\mathbf{J} - \mathbf{s})\right]^{-1} \tag{2.2}$$

For a general ellipsoid, components H_{ijkl} are expressed in terms of elliptic integrals. They reduce to elementary functions for the ellipsoid of revolution (spheroid). Our analysis requires explicit analytic inversions of fourth rank tensors. Such inversions can be done by representing these tensors in terms of a certain "standard" tensorial basis $\mathbf{T}^{(1)}, ..., \mathbf{T}^{(6)}$ [18] (see Appendix):

$$\mathbf{H} = \frac{V_*}{V}\sum_{k=1}^{6} h_k \mathbf{T}^{(k)}; \tag{2.3}$$

so that finding these tensors reduces to calculation of factors h_k. Using the representations for tensors of elastic stiffness, Eshelby's tensor and unit tensor in terms of this basis (Appendix) yields the following relations for the coefficients: Compliance contribution tensor:

$$h_1 = \frac{(\kappa f_0 - f_1)}{2G_0(4\kappa - 1)\left[2\left(\kappa f_0 - f_1\right) - (4\kappa - 1)\, f_0^2\right]};$$

$$h_2 = \frac{1}{2G_0\left[1 - (2 - \kappa)\, f_0 - f_1\right]};$$

$$h_3 = h_4 = \frac{-\left(2\kappa f_0 - f_0 + 2f_1\right)}{4G_0\left(4\kappa - 1\right)\left[2\left(\kappa f_0 - f_1\right) - \left(4\kappa - 1\right) f_0^2\right]}; \tag{2.4}$$

$$h_5 = \frac{4}{4G_0\left[f_0 + 4f_1\right]};$$

$$h_6 = \frac{4\kappa - 1 - 6\kappa f_0 + 2f_0 - 2f}{4G_0\left(4\kappa - 1\right)\left[2\left(\kappa f_0 - f_1\right) - \left(4\kappa - 1\right) f_0^2\right]}$$

Hereafter the following notations are used:

$$\kappa = \frac{1}{2\left(1 - \nu_0\right)}, \qquad f_0 = \frac{\gamma^2\left(1 - g\right)}{2\left(\gamma^2 - 1\right)},$$

$$f_1 = \frac{\kappa\gamma^2}{4\left(\gamma^2 - 1\right)^2}\left[\left(2\gamma^2 + 1\right) g - 3\right] \tag{2.5}$$

where the shape factor g is expressed in terms of aspect ratioγ as follows

$$g(\gamma) = \begin{cases} \frac{1}{\gamma\sqrt{1-\gamma^2}} \arctan\frac{\sqrt{1-\gamma^2}}{\gamma}, & \textit{oblate shape } (\gamma < 1) \\ \frac{1}{2\gamma\sqrt{\gamma^2-1}} \ln\frac{\gamma+\sqrt{\gamma^2-1}}{\gamma-\sqrt{\gamma^2-1}}, & \textit{prolate shape } (\gamma > 1) \end{cases} \tag{2.6}$$

In the case of the overall transverse isotropy, the change in the elastic compliance tensor due to an inhomogeneity has the structure

$$\mathbf{S} - \mathbf{S}_0 == \frac{V_*}{VE_0}\left[W_1\mathbf{II} + W_2 tr\mathbf{J} + \right. \tag{2.7}$$

$$\left. W_3\left(\mathbf{Inn} + \mathbf{nnI}\right) + W_4\left(\mathbf{J}\cdot\mathbf{nn} + \mathbf{nn}\cdot\mathbf{J}\right) + W_5\mathbf{nnnn}\right]$$

where coefficients W_i are expressed in terms of coefficients h_i as follows:

$$W_1 = h_1 - h_2/2; \quad W_2 = h_2; \quad W_3 = 2h_3 + h_2 - 2h_1$$

$$W_4 = h_5 - 2h_2; \quad W_5 = h_6 + h_1 + h_2/2 - 2h_3 - h_5 \tag{2.8}$$

2.2 Resistivity contribution tensors

Utilizing the same approach as the one for the elastic problem, resistivity contribution tensors $\mathbf{H}^C$ can be expressed in terms of Eshelby's tensor for conductivity problem $\mathbf{s}^C$ as follows:

$$\mathbf{H}^C = \frac{V^*}{V}\frac{1}{k_0}\left(\mathbf{I} - \mathbf{s}^C\right)^{-1} \tag{2.9}$$

In the case of the spheroidal pore, tensor $\mathbf{s}^C$ has the following form:

$$\mathbf{s}^K = f_0(\gamma)(\mathbf{I} - \mathbf{nn}) + (1 - 2f_0(\gamma))\,\mathbf{nn} \tag{2.10}$$

where $f_0(\gamma)$is given by (2.9). Substituting this result into (4.2) yields the following expression for $\mathbf{H}^C$

$$H^C = \frac{V^*}{V_0}\frac{1}{k_0}\{A_1\mathbf{I} + A_2\mathbf{nn}\} \tag{2.11}$$

where factors A_1 and A_2 are as follows

$$A_1 = \frac{1}{1 - f_0(\gamma)}, \qquad A_2 = \frac{1 - 3f_0(\gamma)}{2f_0(\gamma)\left[1 - f_0(\gamma)\right]} \tag{2.12}$$

In the case of overall transverse isotropy the change in conductivity due to a pore can be obtained as

$$\mathbf{K}^{-1} - \mathbf{K}_0^{-1} = \frac{V*}{V}\frac{1}{k_0}(\mathbf{I}A_1 + A_2\mathbf{nn}) \tag{2.13}$$

3 Correlation between elastic and electric properties of porous metals

Establishing the sought cross-property correlations crucially depends on the possibility to express, with sufficient accuracy, the compliance contribution tensor of a pore in terms of a certain second rank tensor. The following two issues should be addressed in this context.

(A) For a solid with one pore, we identify the inclusion shapes for which the characterization by $\mathbf{H}$ tensor can be reduced, with sufficient

accuracy, to one in terms of a certain second rank symmetric tensor $\mathbf{\Omega}$:

$$\begin{aligned}\mathbf{H} &= \tfrac{1}{E_0}\tfrac{V_*}{V}\Big[\underbrace{B_1\mathbf{II}+B_2\mathbf{J}}_{isotropic\ terms}+ \\ &B_3\left(\mathbf{\Omega I}+\mathbf{I\Omega}\right)+B_4\left(\mathbf{\Omega}\cdot\mathbf{J}+\mathbf{J}\cdot\mathbf{\Omega}\right)\Big],\end{aligned} \tag{3.1}$$

where B_i are scalar coefficients that depend on the inclusion shape and on the matrix-inclusion elastic contrast. The "isotropic terms" in (3.1) are expressed in terms of the second rank and fourth rank unit tensors ($I_{ij}=\delta_{ij}$ and $2J_{ijkl}=\delta_{ik}\delta_{jl}+\delta_{il}\delta_{jk}$) and, thus, do not depend on the inclusion orientation.

(B) For a solid with many pores (analyzed in the framework of the non-interaction approximation) a similar structure should be established for the sum $\sum \mathbf{H}^{(k)}$.

In the case of axial symmetry of the pore shape (spheroid, for example), the representation (3.1) implies the following restrictions on coefficients h_i:

$$h_6+h_1+h_2 2-2h_3-h_5=0. \tag{3.2}$$

With the trivial exception of a sphere, representations (3.1) do not hold exactly. But condition (3.2) is satisfied, with good accuracy, for spheroids within several ranges of parameters that, being sufficiently wide, are relevant for realistic matrix composites. Indeed, one can construct a fictitious compliance contribution tensor $\hat{\mathbf{H}}$, with coefficients $\hat{h}_i$ in the tensorial basis that are obtained from h_i by multiplication of h_i by either $(1+\delta)$ or $(1-\delta)$, and choose δ in such a way that condition (3.2) is satisfied exactly for $\hat{h}_i$:

$$\begin{aligned}\hat{h}_1 &= h_1\left(1-\delta\ \mathrm{sign}\ h_1\right), \quad \hat{h}_2=h_2\left(1-\delta\ \mathrm{sign}\ h_2\right), \\ \hat{h}_3 &= h_3\left(1+\delta\ \mathrm{sign}\ h_3\right), \quad \hat{h}_5=h_5\left(1+\delta\ \mathrm{sign}\ h_5\right) \\ \hat{h}_6 &= h_6\left(1-\delta\ \mathrm{sign}\ h_6\right),\end{aligned} \tag{3.3}$$

where

$$\delta=\frac{h_6+h_1+h_2/2-2h_3-h_5}{|h_6|+|h_1|+|h_2|/2+2|h_3|+|h|_5}. \tag{3.4}$$

Then we find that the error of this approximation, as estimated by the norm $\max_{ijkl,H_{ijkl}\neq 0}\left|\left(H_{ijkl}-\hat{H}_{ijkl}\right)/H_{ijkl}\right|$, is equal to $|\delta|$. The choice of this norm, as the measure of accuracy of representation (3.1), corresponds to the requirement that strain responses to *all* stress states of the actual and of the fictitious inclusions are close if the norm is small. Fig 1 illustrates dependence of $|\delta|$on the pore aspect ratio and Poisson's ratio of the matrix.

Thus, we obtain the following expressions for coefficients B_i:

$$B_1 = E_0\left(\hat{h}_1 - \hat{h}_2/2\right);\ B_2 = E_0\hat{h}_2$$

$$B_3 = E_0\left(2\hat{h}_3 + \hat{h}_2 - 2\hat{h}_1\right);\ B_4 = E_0\left(\hat{h}_5 - 2\hat{h}_2\right) \tag{3.5}$$

Fig 2, illustrate these coefficients as functions of the inclusion's aspect ratio and of the matrix Poisson's ratio.

For a solid with *many* pores, we seek to approximate the sum (over all inclusions) by the expressions

$$\begin{aligned}\sum H^{(k)} \;=\; & \frac{1}{E_0}\Big[\underbrace{pb_1\mathbf{II}+pb_2\mathbf{J}}_{isotropic\ terms}+ \\ & b_3\left(\omega\mathbf{I}+\mathbf{I}\omega\right)+b_4\left(\omega\cdot\mathbf{J}+\mathbf{J}\cdot\omega\right)\Big]\end{aligned} \tag{3.6}$$

where p is the volume concentration of pores and b_i, are scalar coefficients that depend on the average inclusion shapes, as well as on the Poisson's ratio of the matrix ν_0.

Note that representation (3.1) for *one* inclusion constitutes a necessary, but not a sufficient condition for representation (3.6) to hold (with an important exception of the case when all the inhomogeneities have identical shapes). This is due to the fact that, for *mixtures* of diverse shapes, coefficients B_i entering (3.1) are different for different inhomogeneities. The analysis below shows that, nevertheless, representation (3.6) holds for a wide range of realistic microstructures.

Remark 1 *Aside from being a key point in establishing the cross-property correlations, representation (3.6) (when it is possible) has far reaching implications, as follows [6].*

1. It implies that *a solid with pores is approximately orthotropic* (orthotropy being coaxial with the principal axes of ω). We emphasize that the orthotropy holds for any orientational and aspect ratio distributions of pores, including cases when the orthotropic symmetry does not seem to agree with intuition (like several families of parallel cracks inclined at arbitrary angles to each other).

2. Moreover, the orthotropy due to inclusions is of a special, simplified type. This is due to the fact that the effective compliance tensor $\mathbf{S}$ can be expressed in terms of a symmetric second rank tensor ω.

For a solid with many inclusions, we obtain (in frames of non-interaction approximation), utilizing relations (3.6) and (2.13), the following effective compliances and conductivities:

$$\mathbf{S} = \mathbf{S}_0 + \frac{1}{E_0}\frac{1}{V}\left[\mathbf{II}\sum_i (V * B_1)^{(i)} + \mathbf{J}\sum_i (V * B_2)^{(i)} + \right. \tag{3.7}$$

$$\left. + \left(\mathbf{I}\sum_i (V * B_3\mathbf{nn})^{(i)}\right)_{\text{symm}} + \left(\mathbf{J}\cdot\sum_i (V * B_4\mathbf{nn})^{(i)}\right)_{\text{symm}}\right]$$

$$\mathbf{K}^{-1} - \mathbf{K}_0^{-1} = \frac{1}{Vk_0}\left\{\mathbf{I}\sum_i (V * A_1)^{(i)} + \sum_i (V * A_2\mathbf{nn})^{(i)}\right\} \tag{3.8}$$

where coefficients B_i and A_i are given by (3.5) and (2.12), respectively and the subscript "symm" refers to the symmetrization appropriate for the elasticity tensors.

These formulae apply to an arbitrary mixture of pores of diverse aspect ratios and orientations and contain factors A_i and B_i that depend on the pore shapes. Since these factors are different for different inclusions, tensors $\sum (V^* B_i\mathbf{nn})$ and $\sum (V^* A_2\mathbf{nn})$ entering $\mathbf{S}$ and $\mathbf{K}$, respectively, cannot, generally, be expressed in terms of each other and may not even be coaxial.

However, if pores' aspect ratios are not correlated with either orientations of the pores or their volumes (note that volumes and orientations

may be correlated), coefficients B_i and A_i can be replaced by their averages and taken out of the summation signs (if all the inclusions have the same orientation $\mathbf{n}$, this requirement reduces to the condition that the distributions over shapes and over volumes of the inclusions are uncorrelated). This important case appears to be relevant for realistic microstructures.

Then two tensors $\mathbf{S}$ and $\mathbf{K}$ are expressed in terms of the same second rank symmetric tensor ("porosity tensor"):

$$\omega = \frac{1}{V}\sum_k \left(V_* \mathbf{nn}\right)^{(k)} \tag{3.9}$$

Note that its trace $tr\omega = (1/V)\sum V_*$ is the volume fraction of pores p. Thus,

$$\mathbf{S} = \mathbf{S}_0 + \frac{1}{E_0} p\left(b_1 \mathbf{II} + b_2 \mathbf{J}\right) + \frac{1}{E_0}\left[b_3\left(\omega \mathbf{I} + \mathbf{I}\omega\right) + b_4\left(\omega \cdot \mathbf{J} + \mathbf{J} \cdot \omega\right)\right] \tag{3.10}$$

$$\mathbf{K}^{-1} - \mathbf{K}_0^{-1} = \frac{1}{k_0}\left\{a_1 c \mathbf{I} + a_2 \omega\right\} \tag{3.11}$$

Coefficients b_i and a_i- average shape factors for the elasticity problem and for the conductivity problem, respectively - are averages (over all the cavities) of coefficients B_i and A_i:

$$b_i = \int_0^\infty B_i\left(\gamma\right)\lambda\left(\gamma\right)d\gamma, \qquad a_i = \int_0^\infty A_i\left(\gamma\right)\lambda\left(\gamma\right)d\gamma \tag{3.12}$$

where $\lambda\left(\gamma\right)$ is the shape distribution density. Functions $B_i\left(\gamma\right)$ and $A_i\left(\gamma\right)$, given by (3.5) and (2.12), are illustrated in Figs 2,3.

Remark 2 *The possibility to express elasticity tensor* $\mathbf{S}$ *in terms of symmetric second rank tensor* ω *has interesting physical implications. Besides implying the overall elastic orthotropy for any orientational distribution of pores, it also implies that the orthotropic elastic tensors are coaxial with* ω *and, therefore, are coaxial with the overall conductivity tensor* $\mathbf{K}$*. The accuracy of these statements is determined by the accuracy of representation of* $\mathbf{S}$ *in terms* ω*.*

We now return to cross-property correlations. Expressing porosity tensor ω in terms of $\mathbf{K}$ from (3.11) and substituting it into (3.10) yields a cross-property correlation - a closed form expression of the effective compliance tensor in terms of the effective conductivity tensor:

$$\begin{aligned} E_0\left(\mathbf{S}-\mathbf{S}_0\right) = & \left[\tfrac{b_1a_2-2b_3a_1}{a_2(a_2+3a_1)}\mathbf{II}+\tfrac{b_2a_2-2b_4a_1}{a_2(a_2+3a_1)}\mathbf{J}\right]\left[tr\left(k_0\mathbf{K}^{-1}\right)-3\right]+ \\ & +\tfrac{b_3}{a_2}\left[\left(k_0\mathbf{K}^{-1}-\mathbf{I}\right)\mathbf{I}+\mathbf{I}\left(k_0\mathbf{K}^{-1}-\mathbf{I}\right)\right]+ \\ & +\tfrac{b_4}{a_2}\left[\left(k_0\mathbf{K}^{-1}-\mathbf{I}\right)\cdot\mathbf{J}+\mathbf{J}\cdot\left(k_0\mathbf{K}^{-1}-\mathbf{I}\right)\right]. \end{aligned} \tag{3.13}$$

The expression (3.13) is approximate (due to the approximate character of representations (3.6) of the elasticity tensor in terms of a second rank tensor). The derived cross-property correlation contains *four shape factors* - combinations of a_i and b_i- that depend on the average pore shapes. Their presence reflects the fact that the influence of pore shapes on the elastic and on the conductive effective properties is somewhat different (otherwise, the cross-property correlations would have been inclusion shape-independent).

The utility of the explicit cross-property correlation (3.13) can be viewed as follows. If the effective conductivity tensor $\mathbf{K}$ is known, then the only additional information needed to find the full set of anisotropic effective elastic constants is the knowledge of average pore shapes - factors b_i and a_i and not the orientational distribution. Without the cross-property correlation, tensor $\mathbf{S}$ can be expressed in terms of the porosity tensor ω. However, its knowledge requires a rather detailed information (of the orientational character) on the microstructure and may not be readily available. Utilization of the cross-property correlation makes the knowledge of ω unnecessary.

3.1 Homogeneous material with microcracks

In the case of isotropy (random crack orientations), the explicit cross-property correlations were given by Bristow [1]; in the general anisotropic case, such correlations were derived in [6]. In the latter work, the analysis was done in terms of compliance contribution tensors (**H**-tensors) of cracks. However, the conductivity contribution tensor of crack was used

instead of the resisitvity related one, that may lead to a wrong result at high crack densities. In the case of cracks, both the effective conductivities and the approximate representation of the elastic properties are given in terms of a symmetric second rank crack density tensor

$$\alpha = (1/V) \sum \left(a^3 \mathbf{nn}\right) \tag{3.14}$$

Its first invariant $tr\alpha$ coincides with the conventional scalar crack density $\rho = (1/V) \sum a^3$. In terms of α, the effective conductivity tensor is expressed exactly :

$$K = k_0 \left(I + 8\alpha/3\right)^{-1} \tag{3.15}$$

and the effective compliance tensor $\mathbf{S}$ - approximately as follows:

$$\mathbf{S} = \mathbf{S}_0 + \frac{16\left(1-\nu_0^2\right)}{3\left(2-\nu_0\right)E_0}\left[\alpha_{is} J_{sjkl} + J_{ijks}\alpha_{sl}\right] \tag{3.16}$$

Expressing now α in terms of $\mathbf{K} - \mathbf{K}_0$ from (3.15) and substituting into (3.16) yields the explicit cross-property relation:

$$\mathbf{S} = \mathbf{S}_0 + \frac{2\left(1-\nu_0^2\right)}{\left(2-\nu_0\right)E_0}\left[\left(k_0\mathbf{K}^{-1} - \mathbf{I}\right)\cdot\mathbf{J} + \mathbf{J}\cdot\left(k_0\mathbf{K}^{-1} - \mathbf{I}\right)\right] \tag{3.17}$$

In particular, it implies a very simple one-to-one correspondence between the effective Young's moduli E_i and the principal conductivities k_i in the same directions:

$$\frac{E_0 - E_i}{E_i} = \frac{4\left(1-\nu_0^2\right)}{2-\nu_0}\frac{k_0 - k_i}{k_i} \tag{3.18}$$

Note, that the sensitivity of the factor entering (3.18) to Poisson's ratio is very low (it is 2.00 for both $\nu_0 = 0$ and $\nu_0 = 0.5$, reaching 2.144 for $\nu_0 = 0.27$). Formula (3.18) recovers results of Bristow for the case of effective isotropy.

Remark 3 *A physically important observation is that, as far as the effective conductivities, effective compliances and the cross-property correlations are concerned, strongly oblate pores can be replaced by cracks [6]. Thus, all the relations derived in the present subsection, apply to materials with pores having aspect ratios* $\gamma < 0.15$

3.2 The case of overall isotropy

If the porous material is isotropic (pores are either spherical or randomly oriented), tensor ω is isotropic ($\omega = c\mathbf{I}$) and the cross-property correlation (3.17) takes the following form, that contains only two shape factors - coefficients at **II** and **J**:

$$\mathbf{S} = \mathbf{S}_0 + 5\frac{k_0 - k}{kE_0}\left(\frac{b_1 + b_3}{3a_1 + a_2}II + \frac{b_2 + b_4}{3a_1 + a_2}J\right) \tag{3.19}$$

We note that the overall isotropy takes place in one of the two cases: (A) spherical inclusions and (B) randomly oriented non-spherical inclusions. While in case (A) the cross-property correlation (3.19) becomes exact, in the case (B) it is approximate, since it is based on the approximate representations of tensor **H** in terms of a second rank tensor. However, in case (B), the *exact* cross-property correlation can be derived independently (without using the approximation (3.1)). Indeed, in this case, the exact representation (2.7) of the effective elastic compliance tensor is:

$$\begin{aligned} E_0\left(\mathbf{S} - \mathbf{S}_0\right) &= p\left(w_1 + w_3/3 + w_5/15\right)\mathbf{II} + \\ &\quad c\left(w_2 + w_4/3 + w_5/15\right)\mathbf{J} \end{aligned} \tag{3.20}$$

where w_i are related to W_i for the individual inclusions (given by (2.8)) by formulas analogous to (3.12). The effective conductivity in the case of isotropy takes the form

$$k = k_0/1 - a_1 p - a_2 p/3 \tag{3.21}$$

Solving for the porosity p from (3.21) and substituting into (3.20) yields the exact cross-property correlation for isotropic porous material

$$\begin{aligned} E_0\left(\mathbf{S} - \mathbf{S}_0\right) = \frac{3\left(k_0 - k\right)}{k}\Bigg[&\frac{w_1 + w_3/3 + w_5/15}{3a_1 + a_2}\mathbf{II} + \\ &\frac{w_2 + w_4/3 + w_5/15}{3a_1 + a_2}\mathbf{J}\Bigg] \end{aligned} \tag{3.22}$$

In particular, the effective Young's modulus and Poisson's ratio are exactly expressed in terms of the effective conductivity k as follows:

$$\frac{E_0 - E}{E} = \frac{3\left(w_1 + w_2\right) + w_3 + w_4 + 2w_5/5}{3a_1 + a_2}\frac{k_0 - k}{k} \tag{3.23}$$

$$\nu = \frac{\nu_0 k\,(3a_1 + a_2) - (k_0 - k)\,(3w_1 + w_3 + w_5/5)}{[k\,(3a_1 + a_2) + (k_0 - k)\,(3w_1 + 3w_2 + w_3 + w_4 + 2w_5/5)]}$$

4 Experimental verification

The cross-property correlations were derived in the previous section in the framework of non-interaction approximation. To extend the applicability of the derived correlations to high concentrations of inclusions, we suggest and experimentally verify the following key hypothesis: *interactions between pores affect both groups of properties - elastic and conductive - in a similar way, so that the cross-property correlations derived in the non-interaction approximation continue to hold* (although this approximation may yield substantial errors for each of the properties *separately*). This hypothesis was first suggested by Bristow [1]. In this section we discuss two materials - metal foam and aluminum alloy containing multiple microcracks due to cyclic loading (fatigue damage).

4.1 Metal foam [9]

To verify the theoretical predictions, Young moduli and electric conductivities of AlMgSi foam were measured at various levels of porosity (from 70 to 90%). Then Young's modulus was calculated via electric conductivities and compared with the experimental measurements.

In the case of randomly distributed pores (overall isotropy) that slightly differ from spherical shape (note, that "slightly" allows variation in the aspect ratio from 0.7 to 1.4 [6])

$$\frac{1}{E_{eff}} = \frac{1}{E_0} + \frac{p}{1-p}\frac{3\,(1-\nu_0)\,(9+5\nu_0)}{2\,(7-5\nu_0)} \tag{4.1}$$

and

$$\frac{1}{k_{eff}} = \frac{1}{k_0} + \frac{1}{2k_0}\frac{3p}{1-p} \tag{4.2}$$

Now expressing p from (4.2) and substituting it into (4.1) gives us cross-property correlation for porous material in the form:

$$\frac{E_0 - E_{eff}}{E_{eff}} = \frac{(1-\nu_0)\,(9+5\nu_0)}{(7-5\nu_0)}\frac{k_0 - k_{eff}}{k_{eff}} \tag{4.3}$$

Aluminum foam samples were prepared in Institute of Materials and Machine Mechanics, Slovak Academy of Sciences by the powder metallurgy technique. Two different geometries of the test specimens were used: cylindrical rods with a diameter of 25 mm and length 300 mm (for measuring modulus of elasticity) and flat plates with dimensions 140 x 140 x 8.5 mm (for measuring electrical conductivity). The pores within specimens have usually average radii in the range of 0.5 - 2.5 mm depending on the porosity. The computer analysis of sample cross-section revealed that pores were preferentially oriented parallel to the sample axis/horizontal base with slightly elongated pore shape (see Fig.4a). However, the degree of the anisotropy of electric conductivity was found to be smaller than 10% for porosity higher than 78% and to be smaller than 20% for porosity higher than 63%. Therefore, the sample can be considered as almost isotropic. (see Fig.1).

The electrical conductivity of the flat aluminum foam samples was calculated from the geometry and resistance of the specimens (see Fig.4b). The resistance measurements were performed by the "four point" method in which four sharp tungsten electrodes are positioned under an optical microscope and are mechanically pressed in the sample surface. All the electrodes should be aligned in one line. The outer two electrodes are current bearing while the inner two electrodes in between are used for the voltage tap over the electrode distance. The modulus of elasticity of the foam was determined from free vibrations of the sample (in order to eliminate any plastic deformation during tensile/compression test). The cylindrical specimens were vibrated longitudinally using an "impact hammer" [19] while the frequency response was measured with an accelerometer. The samples' vibration response exhibits amplitude maximum for various resonant frequencies corresponding to harmonic oscillations. The modulus of elasticity (Fig.4c) E is calculated from the resonant frequency f_n according to

$$E = \rho . \left(2L \frac{f_n}{n} \right)^2 , \tag{4.4}$$

where n is the order of the resonant frequency in harmonic oscillation, ρ is the density and L is the length of the specimen.

To verify the cross-property correlation, we substitute the measured values of electric conductivity at various levels of porosity into (4.3)

and compare thus obtained values of E_{eff}/E_0 with experimental measurements. The results of the comparison are presented in Fig.4c. The agreement between the theoretical predictions and experimental measurements is better than 10% for all considered porosity levels as shown in Table 1.

4.2 Microcracked material [10]

Aluminum alloy (Aluminum 2124-T351) samples reinforced with 15%, 20% and 25% volume fraction of particulate of Aluminum 3003-H18 were used for experimental verification of the cross-property correlation for microcracked material. The specimens had geometry of cylindrical rods with a diameter of 25 mm and length 300 mm. The mechanical properties of the matrix and the inclusions almost coincide (see Table 2). The only reason for choosing the composition instead of a homogeneous material is to create stress concentrators at interfaces (due to imperfect contacts) to promote nucleation of microcracks. The specimens were subjected to an axial force. All tests were performed under a strain-controlled mode (1.4% strain). The input signals were generated by a computer program. Through the feedback systems, the axial load was adjusted to maintain the value axial strain reading to that of the initial input signal. Data were recorded in a real time mode by a computer and the hysteresis loop in axial direction was plotted on the monitor (see Fig.5a). The electrical conductivity in the loading direction was calculated from the geometry and resistance of the sample in this direction. The resistance measurement was performed by the "four point" method (described in the previous subsection). The change in electric conductivity is presented in Fig.5b as a function of number of cycles for three different concentrations of inclusions. Note that the decrease in conductivity is bigger for higher inclusion concentrations. The Young's modulus of the specimen along the loading direction was determined from the free vibrations of the sample. To verify formula (3.18), we substitute the measured values of electric conductivity at various numbers of cycles into (3.18) and compare the obtained by such a way values of E_1 with experimental measurements. The results of the comparison are presented in Fig.5c. The agreement between the theoretical prediction and experimental measurements is better than 15% for all considered

values of conductivity. Note, that, the cross-property correlation in the framework of non-int eraction approximation is identical to those derived in the framework of Mori-Tanaka's scheme [20, 21]. Therefore we verified the hypothesis formulated in the beginning of this section - that the interactions affect both groups of properties - elastic and conductive - in a similar way, so that the cross-property correlations derived in the non-interaction approximation continue to hold at high concentrations of the defects although this approximation may yield substantial errors for each of the properties separately.

5 Plastic yield in terms of effective electric conductivities

It is well known that porosity enhances plasticity in elastic-plastic materials (in the sense that the macroscopic plasticity is identified with lower level of stresses). The transversely isotropic yield condition of a porous material has the form [22]:

$$2\tau*^2 = \underbrace{A_1\left(\sigma_{kk}\right)^2 + A_2\tau_{ij}\tau_{ji}}_{\text{isotropic part}} + \underbrace{A_3\left(\sigma_{kk}\right)\sigma_{33} + A_4\sigma_{3j}\sigma_{j3} + A_5\sigma_{33}^2}_{\text{anisotropic part}} \tag{5.1}$$

where τ^* is yield stress of the matrix material and $\tau_{ij} = \sigma_{ij} - (\sigma_{kk}/3)\,\delta_{ij}$ is the stress deviator. In contrast with the dense material, this yield condition is sensitive to the first invariant of stresses σ_{kk} (terms with coefficients A_1 and A_3). In the case of the overall isotropy (spherical pores or randomly oriented non-spherical ones), only the first two terms of (5.1) remain.

Dimensionless factors A_{1-5} are key parameters that depend on the pore shapes. They can be expressed in terms of the compliance contribution tensors of the pores $\hat{H} = \sum H^{(k)}$ [11] as

$$
\begin{aligned}
A_1 &= \tfrac{2G_0}{3(1+\nu_0)}\left(6\left(1-\nu_0\right)\hat{h}_1+6\nu_0\hat{h}_3+\left(1+\nu_0\right)\hat{h}_2\right)+ \\
&\quad \tfrac{2G_0^2}{3}\left[12\hat{h}_1^2+6\hat{h}_3^2-\hat{h}_2^2\right] \\
A_2 &= 1+4G_0\hat{h}_2+4G_0^2\hat{h}_2^2 \\
A_3 &= \tfrac{4G_0}{1+\nu_0}\left[-2\hat{h}_1+\left(1+\nu_0\right)\hat{h}_2+\left(2+\nu_0\right)\hat{h}_3-\nu_0\hat{h}_6\right]+ \\
&\quad 4G_0^2\left[4\hat{h}_1\hat{h}_3+2\hat{h}_3\hat{h}_6-4\hat{h}_1^2+\hat{h}_2^2-2\hat{h}_3^2\right] \\
A_4 &= 4G_0\left(\hat{h}_5-2\hat{h}_2\right)+2G_0^2\left(\hat{h}_5^2-4\hat{h}_2^2\right) \\
A_5 &= 2G_0\left[2\hat{h}_1+\hat{h}_2-4\hat{h}_3-2\hat{h}_5+2\hat{h}_6\right]+ \\
&\quad 2G_0^2\left[4\hat{h}_1^2+\hat{h}_2^2+6\hat{h}_3^2-\hat{h}_5^2+2\hat{h}_6^2-4\hat{h}_3\left(2\hat{h}_1+\hat{h}_6\right)\right]
\end{aligned}
\tag{5.2}
$$

These expressions are verified numerically in [23]. Now let us use the elasticity/conductivity cross-property relation (3.13) in the following form

$$
\begin{aligned}
E_0\hat{\mathbf{H}} &= E_0\left(\mathbf{S}-\mathbf{S}_0\right)=\left(C_1\mathbf{II}+C_2\mathbf{J}\right)\left[k_0 tr\left(\mathbf{K}^{-}1\right)-3\right]+ \\
&\quad C_3\left[\left(k_0\mathbf{K}^{-1}-\mathbf{I}\right)\mathbf{I}+\mathbf{I}\left(k_0\mathbf{K}^{-1}-\mathbf{I}\right)\right]+ \\
&\quad C_4\left[\left(k_0\mathbf{K}^{-1}-\mathbf{I}\right)\cdot\mathbf{J}+\mathbf{J}\cdot\left(k_0\mathbf{K}^{-1}-\mathbf{I}\right)\right],
\end{aligned}
\tag{5.3}
$$

where

$$
C_1=\frac{b_1a_2-2b_3a_1}{a_2\left(a_2+3a_1\right)},\ C_2=\frac{b_2a_2-2b_4a_1}{a_2\left(a_2+3a_1\right)},\ C_3=\frac{b_3}{a_2},\ C_4=\frac{b_4}{a_2} \tag{5.4}
$$

Representing tensor $\hat{\mathbf{H}}$ as a linear combination of six "standard" tensors $\mathbf{T}^{(m)}$ (the "standard" tensorial basis) $\hat{\mathbf{H}}=\sum\limits_{m=1}^{6}\hat{h}_m\mathbf{T}^{(m)}$ we get the following expressions for the coefficients $\hat{h}_m$:

$$
\begin{aligned}
\hat{h}_1 &= (2C_1 + C_2 + 2C_3 + C_4)\,\tfrac{k_0-k_{11}}{k_{11}} + \left(C_1 + \tfrac{1}{2}C_2\right)\tfrac{k_0-k_{33}}{k_{33}} \\
\hat{h}_2 &= 2\,(C_2 + C_4)\,\tfrac{k_0-k_{11}}{k_{11}} + C_2\tfrac{k_0-k_{33}}{k_{33}} \\
\hat{h}_3 &= \hat{h}_4 = (2C_1 + C_3)\,\tfrac{k_0-k_{11}}{k_{11}} + (C_1 + C_3)\,\tfrac{k_0-k_{33}}{k_{33}} \\
\hat{h}_5 &= 2\,(2C_2 + C_4)\,\tfrac{k_0-k_{11}}{k_{11}} + 2\,(C_2 + C_4)\,\tfrac{k_0-k_{33}}{k_{33}} \\
\hat{h}_6 &= 2\,(C_1 + C_2)\,\tfrac{k_0-k_{11}}{k_{11}} + (C_1 + C_2 + 2C_3 + 2C_4)\,\tfrac{k_0-k_{33}}{k_{33}}
\end{aligned}
\tag{5.5}
$$

Substituting now (5.5) into (5.2) expresses the plastic yield factors A_i in terms of the conductivities:

$$
\begin{aligned}
A_1 &= \alpha_{11}\tfrac{k_0-k_{11}}{k_{11}} + \alpha_{12}\tfrac{k_0-k_{33}}{k_{33}} + \alpha_{13}\left(\tfrac{k_0-k_{11}}{k_{11}}\right)^2 + \\
&\quad \alpha_{14}\left(\tfrac{k_0-k_{33}}{k_{33}}\right)^2 + \alpha_{15}\tfrac{k_0-k_{11}}{k_{11}}\tfrac{k_0-k_{33}}{k_{33}}, \\
A_2 &= \alpha_{21}\tfrac{k_0-k_{11}}{k_{11}} + \alpha_{22}\tfrac{k_0-k_{33}}{k_{33}} + \alpha_{23}\left(\tfrac{k_0-k_{11}}{k_{11}}\right)^2 + \\
&\quad \alpha_{24}\left(\tfrac{k_0-k_{33}}{k_{33}}\right)^2 + \alpha_{25}\tfrac{k_0-k_{11}}{k_{11}}\tfrac{k_0-k_{33}}{k_{33}}, \\
A_3 &= \alpha_{31}\tfrac{k_0-k_{11}}{k_{11}} + \alpha_{32}\tfrac{k_0-k_{33}}{k_{33}} + \alpha_{33}\left(\tfrac{k_0-k_{11}}{k_{11}}\right)^2 + \\
&\quad \alpha_{34}\left(\tfrac{k_0-k_{33}}{k_{33}}\right)^2 + \alpha_{35}\tfrac{k_0-k_{11}}{k_{11}}\tfrac{k_0-k_{33}}{k_{33}}, \\
A_4 &= \alpha_{41}\tfrac{k_0-k_{11}}{k_{11}} + \alpha_{42}\tfrac{k_0-k_{33}}{k_{33}} + \alpha_{43}\left(\tfrac{k_0-k_{11}}{k_{11}}\right)^2 + \\
&\quad \alpha_{44}\left(\tfrac{k_0-k_{33}}{k_{33}}\right)^2 + \alpha_{45}\tfrac{k_0-k_{11}}{k_{11}}\tfrac{k_0-k_{33}}{k_{33}}, \\
A_5 &= \alpha_{51}\tfrac{k_0-k_{11}}{k_{11}} + \alpha_{52}\tfrac{k_0-k_{33}}{k_{33}} + \alpha_{53}\left(\tfrac{k_0-k_{11}}{k_{11}}\right)^2 + \\
&\quad \alpha_{54}\left(\tfrac{k_0-k_{33}}{k_{33}}\right)^2 + \alpha_{55}\tfrac{k_0-k_{11}}{k_{11}}\tfrac{k_0-k_{33}}{k_{33}}.
\end{aligned}
\tag{5.6}
$$

These relations contain no adjustable parameters. Dimensionless coefficients α_{ij} depend, in the known way, on the average pore shapes

(via C_{1-4}). The sensitivity to pore shapes is due to the fact that the shapes affect the conductivity and the plastic yield somewhat differently (otherwise, relations (5.6) would have been pore shape - independent).

Pore shape dependence of relations (5.6) is illustrated in Figs 6 and 7. Fig. 6 shows the sensitivity to pore shapes of coefficients α_{ij}. This sensitivity is relatively moderate (and negligible for the coefficients entering A_5). Moreover, in the important limits of strongly oblate (crack-like) and strongly prolate pores (discussed in the text to follow), the curves of Fig.6 become flat, indicating that the sensitivity to the aspect ratio vanishes in these limits.

Fig. 7 gives a numerical example of recovering the plastic yield factors A_i from the conductivity data. It is seen that such a recovery requires an information on the average pore shapes (the curves corresponding to different aspect ratios γ differ significantly).

Remark 4 *Being sensitive to pore shapes, relations (5.6) are not sensitive to the overall porosity p. This is a consequence of the fact that, in the framework of Mori-Tanaka's scheme, p affects the effective elasticity and the effective conductivity in a similar way.*

The utility of relations (5.6) is as follows. *Without* them, A_i can be expressed in terms of coefficients $\hat{h}_m$- characteristics of the pore space. However, $\hat{h}_m$ require knowledge not only of pore shapes, but of their orientational distribution as well, including such details as, for example, the extent of orientational scatter about the dominant orientation. Such information may not be readily available.

Utilization of the cross-property correlation makes this orientational information unnecessary. Indeed, if the conductivities are known, the only additional information needed to construct the yield surface is on the average pore shape. Moreover, in the cases when pores are known to have strongly oblate or strongly prolate shapes, no further information on the porous space geometry is needed.

5.1 Strongly oblate (crack-like) pores

This particular case is of interest, for example, in connection with porous metals that have been subjected to rolling. Expressions (5.5) take the form:

$$\hat{h}_1 = \frac{2\left(1-\nu_0^2\right)}{(2-\nu_0)E}\frac{k_0-k_{11}}{k_{11}}, \quad \hat{h}_2 = \frac{4\left(1-\nu_0^2\right)}{(2-\nu_0)E}\frac{k_0-k_{11}}{k_{11}}$$

$$\hat{h}_3 = \hat{h}_4 = 0, \qquad \hat{h}_5 = \frac{4\left(1-\nu_0^2\right)}{(2-\nu_0)E}\left[\frac{k_0-k_{11}}{k_{11}} + \frac{k_0-k_{33}}{k_{33}}\right], \tag{5.7}$$

$$\hat{h}_6 = \frac{4\left(1-\nu_0^2\right)}{(2-\nu_0)E}\frac{k_0-k_{33}}{k_{33}}$$

and plastic yield factors A_i are expressed in terms of conductivities:

$$\begin{aligned}
A_1 &= \frac{8}{3}\frac{1-\nu_0}{1+\nu_0}\frac{k_0-k_{11}}{k_{11}} + \frac{16}{3}\left(\frac{1-\nu_0}{2-\nu_0}\right)^2\left(\frac{k_0-k_{11}}{k_{11}}\right)^2, \\
A_2 &= 1 + 8\frac{1-\nu_0}{2-\nu_0}\frac{k_0-k_{11}}{k_{11}} + 16\left(\frac{1-\nu_0}{2-\nu_0}\right)^2\left(\frac{k_0-k_{11}}{k_{11}}\right)^2, \\
A_3 &= 8\frac{\nu_0(1-\nu_0)}{(1+\nu_0)(2-\nu_0)}\left(\frac{k_0-k_{11}}{k_{11}} - \frac{k_0-k_{33}}{k_{33}}\right), \\
A_4 &= 8\frac{1-\nu_0}{2-\nu_0}\left(-\frac{k_0-k_{11}}{k_{11}} + \frac{k_0-k_{33}}{k_{33}}\right)\times \\
&\quad \left[1 + \frac{1-\nu_0}{2-\nu_0}\left(3\frac{k_0-k_{11}}{k_{11}} + \frac{k_0-k_{33}}{k_{33}}\right)\right], \\
A_5 &= 8\left(\frac{1-\nu_0}{2-\nu_0}\right)^2\left(\frac{k_0-k_{11}}{k_{11}} - \frac{k_0-k_{33}}{k_{33}}\right)^2.
\end{aligned} \tag{5.8}$$

6 Conclusions

The paper overviews the recently obtained results on correlation between mechanical and conductive properties of porous/microcracked materials published in [6-10]. The derived cross–property correlations interrelate, in the closed form, the effective conductivities and mechanical constants (elastic compliances and plastic yield factors) of anisotropic porous/microcracked materials. They may be valuable for applications, if one property (say, conductivities) is easier to measure than the other one (say, a full set of anisotropic elastic constants). Such correlations may also be used to optimize the microstructure for the best combined

conductive/elastic performance. The derived correlations are approximate. Their accuracy depends on the pore shapes and on the Poisson's ratio of the matrix; it remains good in a relatively wide range of parameter. In this range, the effective elastic properties are approximately orthotropic (for any orientational distribution of pores) and the orthotropy axes are coaxial to the principal axes of conductivity. Our results are given in closed form that explicitly reflects inclusion shapes. They are derived in the non-interaction approximation. However, the experimental verification shows that the interactions affect both groups of properties - elastic and conductive - in a similar way, so that the cross-property correlations derived in the non-interaction approximation continue to hold at high concentrations of the defects although this approximation may yield substantial errors for each of the properties separately. The derived correlations contain factors that depend on the average pore shapes. Their presence reflects the fact that pore shapes affect the elasticity and the conductivity differently; otherwise, the correlations would have been universal, independent of microgeometries. However, the information on the microstructure that is reflected in these factors is much less detailed than the one required for a *direct* expression of the effective properties in terms of the microstructure (for example, knowledge of the orientational distribution of pores is not needed). The practical utility of the derived cross-property correlations lies precisely in this fact: if the conductivities (or elastic constants) have been measured, then the microstructural information needed to estimate the elastic constants (or conductivities) is rather minimal and approximate. A methodology is suggested to construct anisotropic plastic yield surfaces of porous metals in terms of electric conductivities. In [11] the yield surfaces is constructed in terms of the porous space geometry (including the orientational distribution). However, this information may not be readily available (particularly the information on details of the orientational distribution of pores, like the orientational scatter about a certain preferred orientation). The methodology proposed here requires the knowledge of conductivities plus an estimate of the average pore shapes. This information on the pore space geometry is rather minimal. Moreover, in the cases when pores are known be strongly oblate or strongly prolate, no further information on pores is required. The conductivity-yield relations derived here hold if (1) material in the ab-

sence of pores ("dense" material) has a clearly identifiable yield point, followed by a horizontal plateau, and (2) the porosity is of the order of 15% or lower.

References

[1] J.R.Bristow, Microcracks, and the static and dynamic elastic constants of annealed heavily cold-worked metals. British J. Appl. Phys, 11, (1960), 81-85.

[2] J.G. Berryman and G.W. Milton, Microgeometry of random composites and porous media. J. Phys., D 21, (1988), 87-94.

[3] L.V. Gibiansky and S. Torquato, Connection between the conductivity and bulk modulus of isotropic composite materials. Phyl. Trans. Roy. Soc .L., A353, (1995), 243-278.

[4] L.V. Gibiansky and S. Torquato, Rigorous link between the conductivity and elastic moduli of fiber reinforced materials. Proc. Roy. Soc. A452, (1996), 253-283.

[5] L.V. Gibiansky and S. Torquato, Bounds on the effective moduli of cracked materials. J Mech Phys Solids 44, (1996), 233-242.

[6] M. Kachanov, I. Sevostianov and B. Shafiro, B. Explicit cross-property correlations for porous materials with anisotropic microstructures, J Mech Phys Solids, 49, (2001), 1-25.

[7] I. Sevostianov and M. Kachanov Explicit cross-property correlations for anisotropic two-phase composite materials. J Mech Phys Solids, 50, (2002), 253-282.

[8] I. Sevostianov., V.E.Verijenko, and M. Kachanov, Cross-property correlations for short fiber reinforced composites with damage and their experimental verification. Composites, B 33, (2002), 205-213.

[9] I. Sevostianov, J. Kovácik, and F. Simancík, Cross-property correlation for metal foams: theory and experiment. Int. J. Frac., 114, (2001), L23-L28.

[10] I. Sevostianov, M. Bogarapu. and P. Tabakov, Correlation between elastic and electric properties for cyclically loaded metals. Int. J. Frac., 115, (2001), L15-L20.

[11] I. Sevostianov and M. Kachanov, On the yield condition for anisotropic porous materials. Int. J. Mater. Sci. Eng., A 313, (2001), 1-15.

[12] V.M. Levin, On the coefficients of thermal expansion of heterogeneous material, Mechanics of Solids, 2, (1967), 58-61.

[13] G.W. Milton, Bounds on the electromagnetic, elastic and other properties of two-component composites. Phys. Rev. Lett., 46, (1981),542-545.

[14] A.V. Cherkaev and L.V. Gibiansky The exact coupled bounds for effective tensors of electrical and magnetic properties of two-component two-dimensional composites. Proc. Roy. Soc. Edinburgh, A122, (1992), 93-125.

[15] G.W. Milton, Composites: a myriad of microstructure independent relations. In: Theoretical and Applied Mechanics 1996, Ed.:Tatsumi, T. et al, Elsevier, Amsterdam, (1997), 443-459.

[16] K.Z. Markov, Elementary micromechanics of heterogeneous media. In: Heterogeneous Media: Micromechanics Modeling Methods and Simulations, ed. K.Z. Markov and L. Preziosi, Birkhauser, (1999), 1-162.

[17] I. Sevostianov and M. Kachanov, Compliance tensor of ellipsoidal inclusions, Int. J. Frac., 96, (1999), L3-L7.

[18] I.A. Kunin, Elastic media with microstructure, Springer Verlag, Berlin, 1983.

[19] Bruel and Kjaer, Mechanical Vibration and Shock Measurements, K. Larsen & Son, Soborg 1980.

[20] T. Mori and K. Tanaka Average stress in matrix and average elastic energy of materials with misfitting inclusions, Acta Met., 21, (1973), 571-574.

[21] Y. Benveniste, On the Mori-Tanaka method for cracked solids, Mech. Res. Comm., 13, (1986), 193-201.

[22] Druyanov, B. Technological Mechanics of Porous Bodies, Clarendon Press, Oxford, 1993

[23] T. Zohdi, M. Kachanov, and I. Sevostianov, A microscale numerical analysis of a plastic flow in a porous material. Int. J. Plasticity (2002, in press).

Appendix A. Tensorial basis in the space of transversely isotropic fourth rank tensors. Representation of certain transversely isotropic tensors in terms of the tensorial basis

The operations of analytic inversion and multiplication of fourth rank tensors are conveniently done in terms of special tensorial bases that are formed by combinations of unit tensor δ_{ij} and one or two orthogonal unit vectors (see Kunin, 1983 and Kanaun and Levin, 1993). In the case of the transversely isotropic elastic symmetry, the following basis is most convenient (it differs slightly from the one used by Kanaun and Levin, 1993):

$$T^{(1)}_{ijkl} = \theta_{ij}\theta_{kl},\ T^{(2)}_{ijkl} = (\theta_{ik}\theta_{lj} + \theta_{il}\theta_{kj} - \theta_{ij}\theta_{kl})/2,$$

$$T^{(3)}_{ijkl} = \theta_{ij}m_k m_l,\ T^{(4)}_{ijkl} = m_i m_j \theta_{kl}$$

$$T^{(5)}_{ijkl} = (\theta_{ik}m_l m_j + \theta_{il}m_k m_j + \theta_{jk}m_l m_i + \theta_{jl}m_k m_i)\,/4,$$

$$T^{(6)}_{ijkl} = m_i m_j m_k m_l \qquad (A.1)$$

where $\theta_{ij} = \delta_{ij} - m_i m_j$ and $m = m_1 e_1 + m_2 e_2 + m_3 e_3$ is a unit vector along the axis of transverse symmetry. These tensors form the closed algebra with respect to the operation of (non-commutative) multiplication (contraction over two indices):

$$\left(\mathbf{T}^{(\alpha)} : \mathbf{T}^{(\beta)}\right)_{ijkl} \equiv T^{(\alpha)}_{ijpq} T^{(\beta)}_{pqkl} \qquad (A.2)$$

The table of multiplication of these tensors has the following form (the column represents the left multipliers):

	$\mathrm{T}^{(1)}$	$\mathrm{T}^{(2)}$	$\mathrm{T}^{(3)}$	$\mathrm{T}^{(4)}$	$\mathrm{T}^{(5)}$	$\mathrm{T}^{(6)}$
$\mathrm{T}^{(1)}$	$2\mathrm{T}^{(1)}$	0	$2\mathrm{T}^{(3)}$	0	0	0
$\mathrm{T}^{(2)}$	0	$\mathrm{T}^{(2)}$	0	0	0	0
$\mathrm{T}^{(3)}$	0	0	0	$\mathrm{T}^{(1)}$	0	$\mathrm{T}^{(3)}$
$\mathrm{T}^{(4)}$	$2\mathrm{T}^{(4)}$	0	$2\mathrm{T}^{(6)}$	0	0	0
$\mathrm{T}^{(5)}$	0	0	0	0	$\mathrm{T}^{(5)}/2$	0
$\mathrm{T}^{(6)}$	0	0	0	$\mathrm{T}^{(4)}$	0	$\mathrm{T}^{(6)}$

Then the inverse of any fourth rank tensor $\mathbf{X}$, as well as the product $\mathbf{X} : \mathbf{Y}$ of two such tensors are readily found in the closed form, as soon as the representation in the basis

$$\mathbf{X} = \sum_{k=1}^{6} X_k \mathbf{T}^{(k)},\ \mathbf{Y} = \sum_{k=1}^{6} Y_k \mathbf{T}^{(k)} \tag{A.3}$$

are established. Indeed:

a) inverse tensor X^{-1}defined by $X^{-1}_{ijmn} X_{mnkl} = \left(X_{ijmn} X^{-1}_{mnkl}\right) = J_{ijkl}$ is given by

$$\mathbf{X}^{-1} = \frac{X_6}{2\Delta}\mathbf{T}^{(1)} + \frac{1}{X_2}\mathbf{T}^{(2)} - \frac{X_3}{\Delta}\mathbf{T}^{(3)} - \frac{X_4}{\Delta}\mathbf{T}^{(4)} + \frac{4}{X_5}\mathbf{T}^{(5)} + \frac{2X_1}{\Delta}\mathbf{T}^{(6)} \tag{A.4}$$

where $\Delta = 2\left(X_1 X_6 - X_3 X_4\right)$.

b) product of two tensors $\mathbf{X} : \mathbf{Y}$ (tensor with $ijkl$ components equal to $X_{ijmn} Y_{mnkl}$) is

$$\mathbf{X} : \mathbf{Y} = \left(2X_1 Y_1 + X_3 Y_4\right)\mathbf{T}^{(1)} + X_2 Y_2 \mathbf{T}^{(2)} + \left(2X_1 Y_3 + X_3 Y_6\right)\mathbf{T}^{(3)} +$$

$$+ \left(2X_4 Y_1 + X_6 Y_4\right)\mathbf{T}^{(4)} + \frac{1}{2} X_5 Y_5 \mathbf{T}^{(5)} + \left(X_6 Y_6 + 2X_4 Y_3\right)\mathbf{T}^{(6)} \tag{A.5}$$

If x_3 is the axis of transverse symmetry, tensors $\mathbf{T}^{(1)}, ..., \mathbf{T}^{(6)}$ given by (A1) have the following non-zero components:

$$T^{(1)}_{1111} = T^{(1)}_{2222} = T^{(1)}_{1122} = T^{(1)}_{2211} = 1$$

$$T^{(2)}_{1212} = T^{(2)}_{2121} = T^{(2)}_{1221} = T^{(2)}_{2112} = T^{(2)}_{1111} = T^{(2)}_{2222} = \frac{1}{2}$$
$$T^{(2)}_{1122} = T^{(2)}_{2211} = -\frac{1}{2}$$
$$T^{(3)}_{1133} = T^{(3)}_{2233} = 1 \qquad (A.6)$$
$$T^{(4)}_{3311} = T^{(4)}_{3322} = 1$$

$$T^{(5)}_{1313} = T^{(5)}_{2323} = T^{(5)}_{1331} = T^{(5)}_{2332} = T^{(5)}_{3113} = T^{(5)}_{3223} = T^{(5)}_{3131} = T^{(5)}_{3232} = \frac{1}{4}$$

$$T^{(6)}_{3333} = 1$$

General transversely isotropic fourth-rank tensor, being represented in this basis

$$\Psi_{ijkl} = \sum \psi_m T^m_{ijkl}$$

has the following components:

$$\psi_1 = (\Psi_{1111} + \Psi_{1122})/2,\ \psi_2 = 2\Psi_{1212}, \psi_3 = \Psi_{1133},\ \psi_4 = \Psi_{3311} \qquad (A.7)$$
$$\psi_5 = 4\Psi_{1313},\ \psi_6 = \Psi_{3333}$$

Utilizing (A.7) one obtains the following representations:

- Tensor of elastic compliances of the isotropic material $S_{ijkl} = \sum s_m T^m_{ijkl}$ has the following components

$$s_1 = \frac{1-\nu}{4G(1+\nu)},\ s_2 = \frac{1}{2G},$$
$$s_3 = s_4 = \frac{-\nu}{2G(1+\nu)},\ s_5 = \frac{1}{G},\ s_6 = \frac{1}{2G(1+\nu)} \qquad (A.8)$$

- Tensor of elastic stiffness of the isotropic material by $C_{ijkl} = \sum c_m T^m_{ijkl}$ has components

$$c_1 = \lambda + G,\ c_2 = 2G,\ c_3 = c_4 = \lambda,\ c_5 = 4G,\ c_6 = \lambda + 2G \quad (A.9)$$

where $\lambda = 2G\nu/(1-2\nu)$.

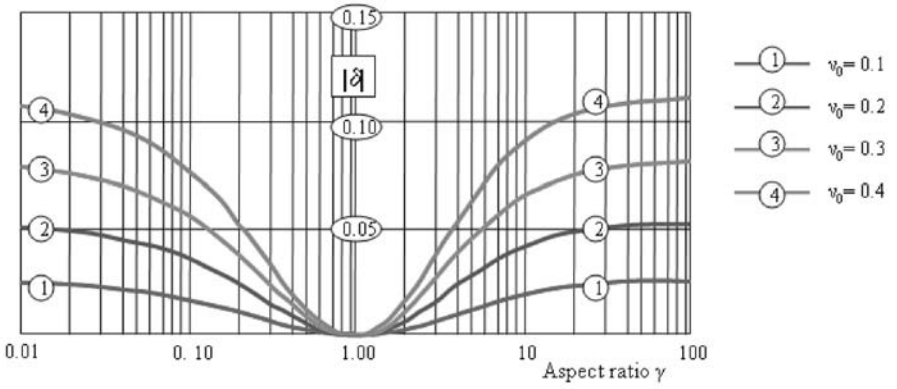

Figure 1: Accuracy of the approximate representation of the pore compliance tensor $\mathbf{H}$ as a function of pore aspect ratio γ for several values of ν_0

- Unit fourth rank tensors are represented in the form

$$J^{(1)}_{ijkl} = (\delta_{ik}\delta_{lj} + \delta_{il}\delta_{kj})/2 = \frac{1}{2}T^1_{ijkl} + T^2_{ijkl} + 2T^5_{ijkl} + T^6_{ijkl} \quad (A.10)$$

$$J^{(2)}_{ijkl} = \delta_{ij}\delta_{kl} = T^1_{ijkl} + T^3_{ijkl} + T^4_{ijkl} + T^6_{ijkl} \quad (A.12)$$

- Eshelby's tensor for spheroidal inclusion $s_{ijkl} = \sum s^e_m T^m_{ijkl}$ has components

$$s^e_1 = \frac{1}{2\,(1-\nu)}f_0 + f_1, \quad s^e_2 = \frac{3-4\nu}{2\,(1-\nu)}f_0 + f_1,$$

$$s^e_3 = \frac{\nu}{1-\nu}f_0 - 2f_1,\ s^e_4 = \frac{\nu}{1-\nu}\,(1-2f_0) - 2f_1, \quad (A.12)$$

$$s^e_5 = 2\,(1-f_0-4f_1)\,, \quad s^e_6 = 1 - 2f_0 + 4f_1,$$

where f_0 and f_1 are given by (2.5).

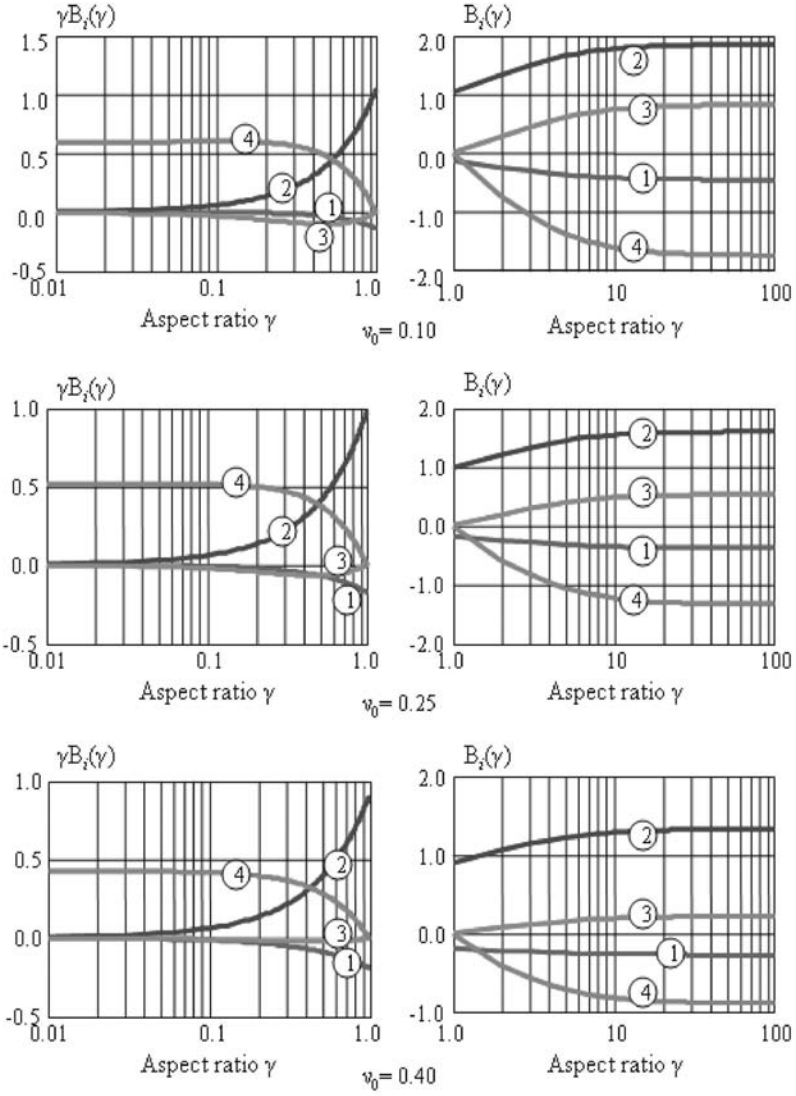

Figure 2: Factors entering approximate expression (3.1) for the compliance contribution tensor **H** as functions of pore aspect ratio γ and Poisson's ratio of the matrix ν_0. Curves 1, 2, 3, and 4 correspond to B_1, B_2,B_3, and B_4. For oblate shapes ($\gamma < 1$) factors B_i enter in product with pore aspect ratio γ, to avoid degeneracy for small γ

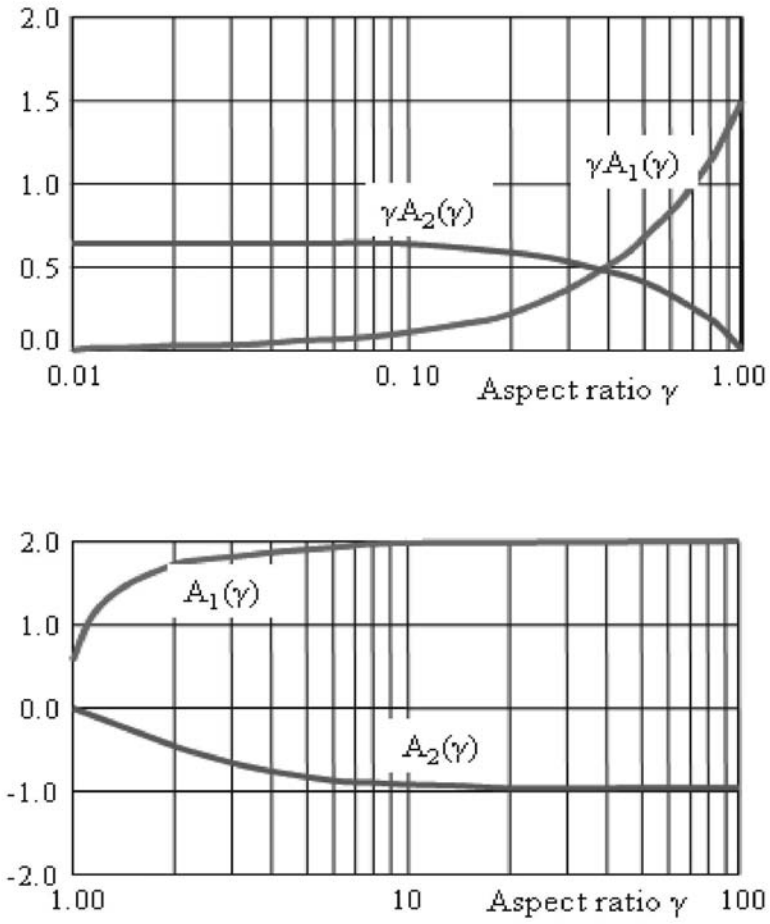

Figure 3: Factors entering expression (2.11) for the resistivity contribution tensor as functions of pore's aspect ratio γ. For oblate shapes ($\gamma < 1$) factors A_i enter in product with pore aspect ratio γ, to avoid degeneracy for small γ

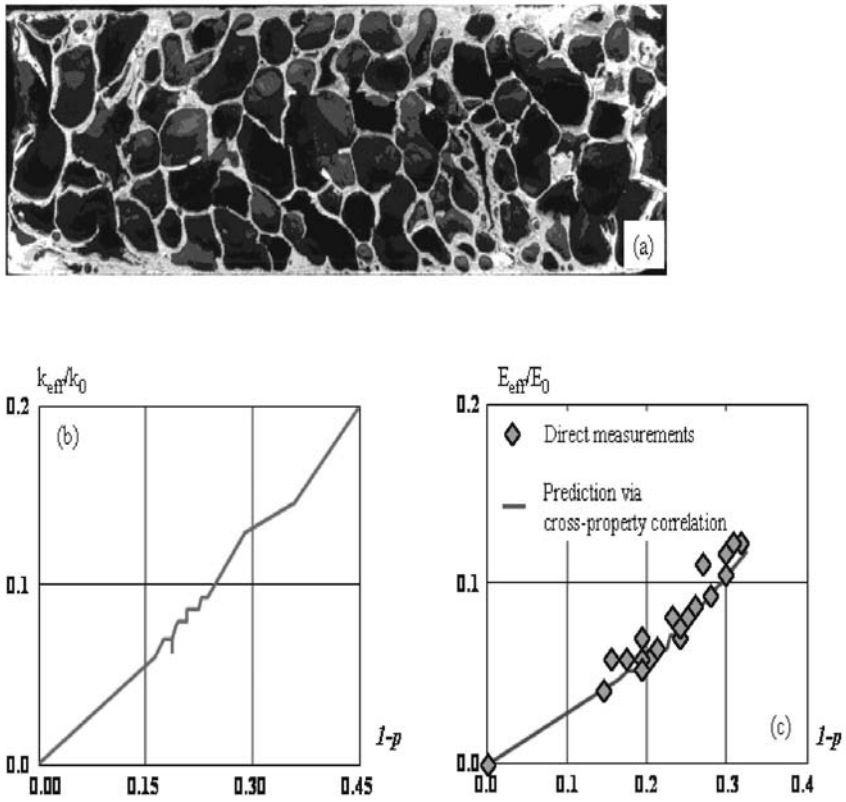

Figure 4: Cross-property correlation for aluminum foam. (a) A typical cross-section of AlMg1Si0.6 aluminum foam; (b) Electric conductivity of aluminum foam as a function of $(1-p)$; (c) Comparison of Young's modulus of aluminum foam calculated via cross-property correlation with experimental measurements

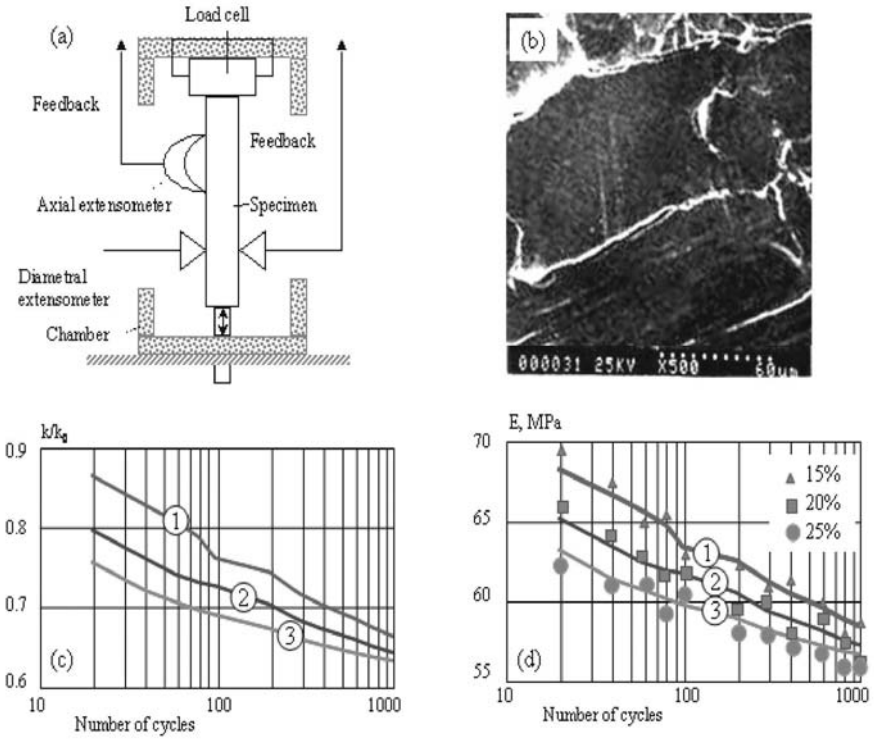

Figure 5: Fatigue experiment. (a) A schematic diagram of the experiment set-up; (b) A typical cross-section of the Al alloys composition subjected to cyclic loading; (c) Change in electric conductivity as a function of loading cycles number for different volume concentrations of inclusions (1- 15%, 2 - 20%, 3 - 25%); (d) Change in Young's modulus as a function of loading cycles number for different volume concentrations of inclusions (1- 15%, 2 - 20%, 3 - 25%): theoretical predictions and experimental measurements

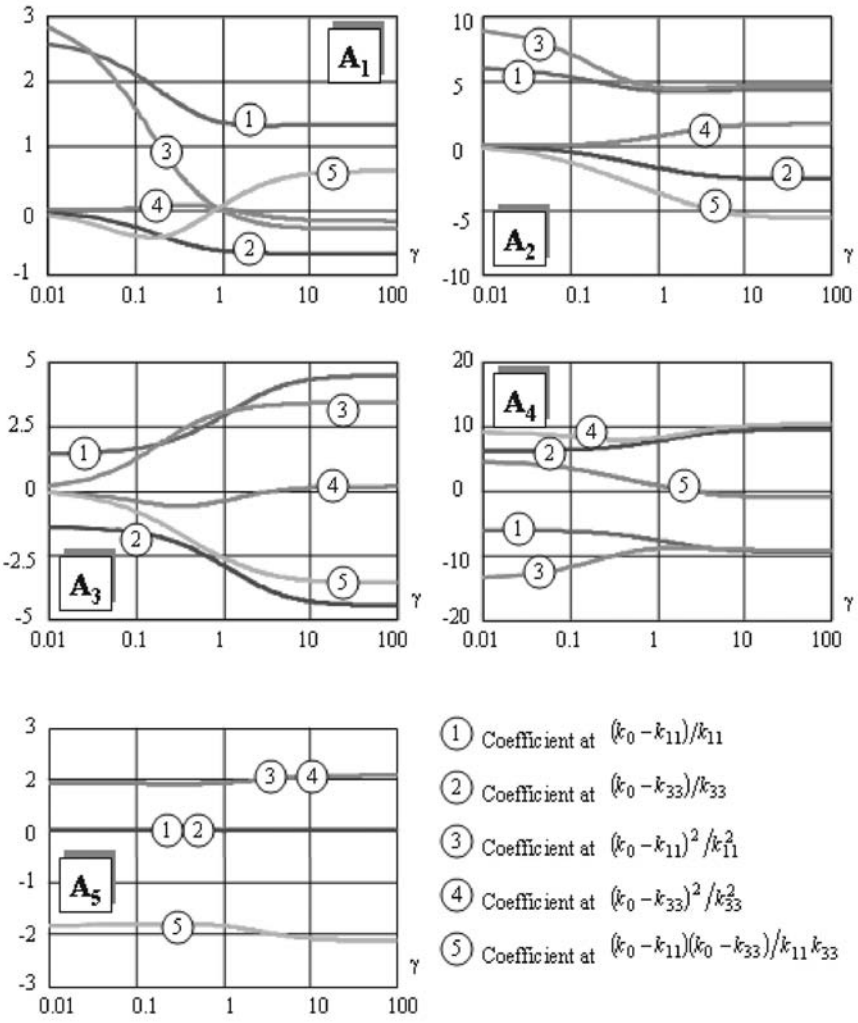

Figure 6: Dependence of coefficients α_{ij} entering plastic yield factors A_i on the average pore aspect ratio γ

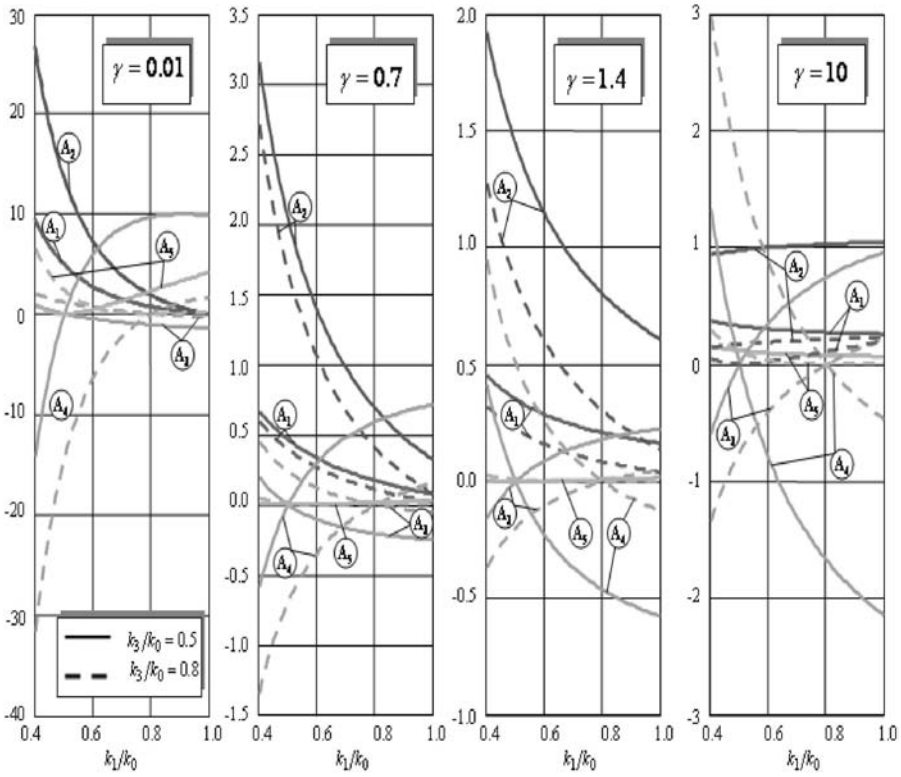

Figure 7: Plastic yield factors A_i in terms of conductivities, for various average pore aspect ratios γ (a numerical example)

P,%	0.84	0.82	0.80	0.79	0.77	0.76	0.71	0.00
k_{eff} $\times 10^6$ S/m	2.23	2.58	2.77	3.23	3.50	3.48	4.83	37.6
E_{eff} -experiment,GPa	3.20	3.86	3.81	4.98	5.48	5.50	7.07	70.0
E_{eff} -theory, GPa	3.46	3.66	3.94	4.61	5.00	4.96	6.96	70.0
Disagreement	7.5%	5.2%	3.3%	7.4%	8.8%	9.6%	1.8%	

Table 1. Comparison of the experimentally measured Young's modulus with calculated via effective electric conductivity with cross-property correlation at various levels of porosity p.

	Young's modulus	*Poisson's ratio*	*Yield strength*	*Electrical conductivity*	*Melting point*	Density
Aluminum 2124-T351	73 GPa	0.33	325 MPa	22.7 MS/m	773 K	2.78
Aluminum 3003-H18	69 GPa	0.33	185 MPa	23.3 MS/m	916 K	2.73

Table 2. Material properties of the constituentsof aluminum alloy composition used in fatigue experiments: Aluminum 2124-T351 (matrix) and Aluminum 3003-H18 (inclusions)

Korelacija izmedju mehaničkih i konduktivnih osobina metala poroznoih ili sa mikroprslinama

UDK 531.01, 537.634, 539.42

Različite fizičke osobine anizotropnih materijala poroznoih ili sa mikroprslinama - posebno elastične i konduktivne - mogu se eksplicitno povezati. Praktična korist ovakvih relacija leži u činjenici da se jedna osobina (recimo, električna provodnost) može lakše meriti od neke druge (recimo, celog skupa anizotropnih elastičnih konstanata). Još jedna primena su veštačke mikrostructure dizajnirane za optimalnu *elastično-provodnu svrhu*. Ove su relacije, izvedene iz mikromehaničkih razmatranja, potvrdjene eksperimentima na nekoliko heterogenih materijala. Pokazano je, takodje, da se anizotropna površ tečenja za neki porozni žilavi materijal može konstruisati iz merenja efektivnih električnih provodnosti. Izvedene unakrsne korelacije osobina su osetljive na količnike aspekta pora i Poisson-ove koeficijente devičanskih materijala.